Biophysical Journal Volume 87 August 2004 745–753

Signaling in Small Subcellular Volumes. II. Stochastic and Diffusion Effects on Synaptic Network Properties

Upinder S. Bhalla

National Centre for Biological Sciences, Tata Institute of Fundamental Research, GKVK Campus, Bangalore, India

ABSTRACT The synaptic signaling network is capable of sophisticated cellular computations. These include the ability to respond selectively to different patterns of input, and to sustain changes in response over long periods. The small volume of the synapse complicates the analysis of signaling because the chemical environment is strongly affected by diffusion and stochasticity. This study is based on an updated version of a previously proposed synaptic signaling circuit (Bhalla and Iyengar, 1999) and analyzes three network computation properties in small volumes: bistability, thresholding, and pattern selectivity. Simulations show that although there are diffusive regimes in which bistability may persist, chemical noise at small volumes overwhelms bistability. In the deterministic situation, the network exhibits a sharp threshold for transition between lower and upper stable states. This transition is broadened and individual runs partition between lower and upper states, when stochasticity is considered. The third network property, pattern selectivity, is severely degraded at synaptic volumes. However, there are regimes in which a process similar to stochastic resonance operates and amplifies pattern selectivity. These results imply that simple scaling of signaling conditions to femtoliter volumes is unlikely, and microenvironments, such as reaction complex formation, may be essential for reliable small-volume signaling.

INTRODUCTION

The synaptic signaling network exhibits several interesting computational functions central to its role in synaptic plasticity. The synapse can manifest plasticity in several ways, but it seems that sustained responses are triggered from rather brief inputs. Further, the temporal pattern of input appears to be the determining factor for deciding which form of plasticity will be expressed (Sheng and Kim, 2002; Tsodyks, 2002). In computational terms, the long-term maintenance of plastic changes requires some form of multistability; the requirement for certain minimal stimuli implies a thresholding process, and these are triggered based on some form of input pattern selectivity. This study analyzes the impact of small volume effects of diffusion and stochasticity on these three computational functions of synaptic signaling.

The synapse contains a complex signaling network which has at least a hundred candidate proteins (Sheng and Kim, 2002). Some of the implicated kinases have been assigned major roles in plasticity. The calcium-calmodulin activated Type II kinase (CaMKII) signaling pathway has been proposed to be involved in long-term information storage (Lisman and McIntyre, 2001). The mitogen-activated protein kinase (MAPK) pathway appears to play a role in stimulus decoding and triggering of nuclear transcriptional effects that are required for long-term synaptic plasticity (Bolshakov et al., 2000; Selcher et al., 2003). The kinases protein kinase C (PKC) and protein kinase A (PKA) also appear to play prominent roles (Abeliovich et al., 1993; Blitzer et al., 1998). A network including these four pathways was the basis of the current study. A similar network model has previously been used to analyze emergent properties of synaptic signaling including bistability and thresholding (Bhalla and Iyengar, 1999; Bhalla, 2002b). Many other studies have focused on different synaptic signaling molecules, especially the CaMKII pathway which has also been proposed to exhibit bistability (Lisman and McIntyre, 2001). Temporal tuning has also been considered using a similar network model (Bhalla, 2002a,b). This study suggests that the synaptic network is capable of quite complex pattern discrimination, and that patterns in the range of seconds to many minutes can in principle be discriminated by the network.

Most of these studies have considered biochemical signaling in the mass-action, nondiffusive limit. Stochasticity introduces complications into the analysis of stability, as fluctuations can spontaneously lead to a flipping of states in a system which is bistable in the deterministic limit. Previous studies have analyzed the biochemical requirements for long-term stability despite such fluctuations (Lisman and Goldring, 1988; Bialek, 2001). These studies have established that bistability is in principle feasible at the molecular complex level, with special reference to the CaMKII autophosphorylation loop. The integrated functioning of multiple signaling pathways of the synaptic network under small-volume conditions has not been analyzed in detail. Further, the computational limitations of such complex reaction-diffusion networks at small volumes remain to be fully explored. This exploration was a major goal of this study.

Submitted January 21, 2004, and accepted for publication April 9, 2004.

Address reprint requests to Upinder S. Bhalla, National Center for Biological Sciences, TIFR, GKVK Campus, Bangalore 560065, India. Tel.: 91-80-2363-6420 ext. 3230; Fax: 91-80-2363-6662; E-mail: bhalla@ncbs.res.in.

0006-3495/04/08/745/09 $2.00

doi: 10.1529/biophysj.104.040501

METHODS

The modeled signaling network included the four individual pathways modeled in the accompanying article as well as some additional pathways involved in interactions with the major kinase pathways. As before, simulation models were derived closely from those used previously to study temporal tuning by signaling networks, and utilized biochemical parameters particularly from neuronal sources (Bhalla, 2002a). A block diagram of the signaling network is presented in Fig. 1 *A*. The full model includes 134 molecules, 80 reactions, and 62 irreversible Michaelis-Menten enzymatic reactions. Most of the reaction steps of the constituent pathways are identical to those in the accompanying article. A few activation steps have been removed for the receptor activation of G-protein type s and the adenylyl cyclase pathway, as these inputs are not used in the current simulations. As before, membrane-bound molecules were treated as nondiffusive, whereas the remaining molecules were treated as diffusing with the same rate for all molecules. The detailed reaction schemes and rate constants have been uploaded to the DOQCS database (Sivakumaran et al., 2003) (http://doqcs.ncbs.res.in) as accession 50 and are presented in the supplementary material. Demonstration scripts for replicating the tests are accessible from within the accessions and from http://www.ncbs.res.in/~bhalla/stochnet/index.html.

Simulation methods were identical to those described in the previous article. Briefly, simulations were run on a 32-CPU cluster (Atipa Technologies, Lawrence, KS) running GENESIS/kinetikit (Bhalla, 1998,2002c). Stochastic calculations were performed using the adaptive stochastic method implemented in recent versions of GENESIS (Vasudeva and Bhalla, 2004). A typical simulation run on a single node took a day to model 7200 s of simulated time. Runs were repeated multiple times and/or on multiple nodes to build up response statistics.

Simulations were done in two geometries. Bistability tests were done using a synaptic spine geometry having a 0.1 fl head and a neck with 1 μm length and 0.01 μm^2 cross-sectional area (Fig. 1 *B*). The spine neck was considered purely as a diffusive barrier and its volume was not considered. Thresholding simulations were performed using the compartmental geometry, where a cubic cellular compartment in the range of 0.1–1000 fl was attached to a bulk volume of 1000 fl. Simulations of temporal tuning were carried out using both geometries. In each case a range of diffusion constants from 10–0.001 μm^2/s were considered. As the diffusion flux depends both on the spine geometry and on the diffusion constant, this wide range of diffusion constants should account for most synaptic contexts. Also, the two geometries are mathematically equivalent with appropriate diffusion scaling, except for the fact that the bulk volume was 1000 fl, whereas the dendritic volume was 1 fl in most runs.

As described in the accompanying article, calcium stimuli were treated as being mediated through a stochastic reaction input to the intracellular calcium pool to generate a more plausible distribution of Ca^{2+} levels. The exception was in the case of the temporal tuning simulations, where Ca^{2+} was simply numerically buffered to the desired level. This approximation was assessed by repeating one of the stimulus conditions using the stochastic reaction input for Ca^{2+}, and it was found that the distributions of responses were statistically indistinguishable.

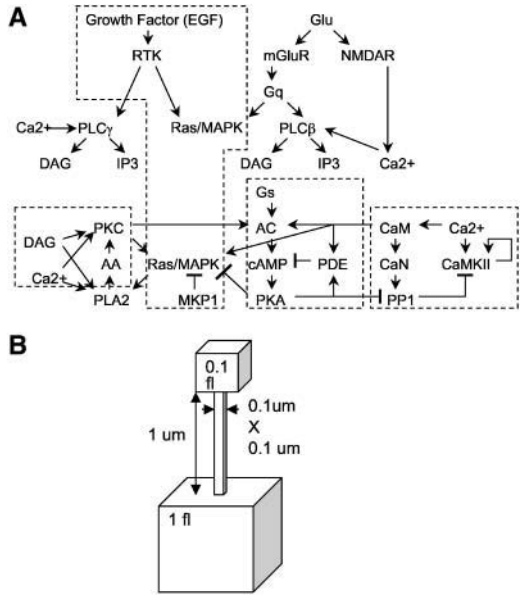

FIGURE 1 Model description. (*A*) Block diagram of signaling network. The dashed lines enclose kinase pathways modeled in the accompanying article. Abbreviations: EGF, epidermal growth factor; RTK, receptor tyrosine kinase; MAPK, mitogen activated protein kinase; MKP1, MAPK phosphatase type 1; Glu, glutamate; mGluR, metabotropic glutamate receptor; NMDAR, *N*-methyl D-aspartate receptor; Gq, G-protein type q; PLCβ, phospholipase C type β; DAG, diacylglycerol; IP3, inositol trisphosphate; PLCγ, phospholipase C type γ; PLA_2, phospholipase A_2; Gs, G-protein type s; AC, adenylyl cyclase; cAMP, cyclic adenosine monophosphate; PDE, phosphodiesterase; PKA, protein kinase A; CaM, calcium calmodulin; CaN, calcineurin; PP1, protein phosphatase 1; CaMKII, calcium calmodulin activated type II kinase. (*B*) Geometry of spine used in simulations. In some cases, as mentioned in the text, the spine head and dendrite volumes were scaled to different volumes.

RESULTS

Bistability and diffusion

Positive feedback loops in signaling networks have the potential to exhibit bistable behavior, where the network can remain in either of two steady states, differing in activity levels (Lisman and McIntyre, 2001). The current model incorporates a positive feedback loop involving MAPK, phospholipase A2 (PLA2), and PKC, which has been shown to be potentially bistable (Bhalla et al., 2002). Bistability ranges for the MAPK-PLA2-PKC feedback loop were assessed using deterministic calculations for different values of diffusion constant and volume. For each condition, the presence of bistability was inferred by constructing a dose-response curve of PKC versus MAPK, and a curve for MAPK versus PKC. The activated form of MAPK is represented as MAPK*. When these curves are plotted on the same axes, their intersection points define the stable points of the system. A bistable system has three intersection points: a lower and upper stable point, and an intermediate metastable (threshold) point (Fig. 2 *A*). If the system is not bistable, there is only a single stable intersection point (Fig. 2 *B*). Using this criterion a state diagram was constructed for the two-compartment and synaptic geometries, respectively (Fig. 2, *C* and *D*). As expected, at high diffusion rate or small volume the washout of signaling components removes bistability. In our model, the spine geometry with a head size of 0.1 fl is bistable only if the diffusion constant is rather low, at 0.01 μm^2/s. Free diffusion constants for proteins are typically in the range of 1–10 μm^2/s (Bray, 2001), though cellular rates may be slower (Weiss et al., 2003).

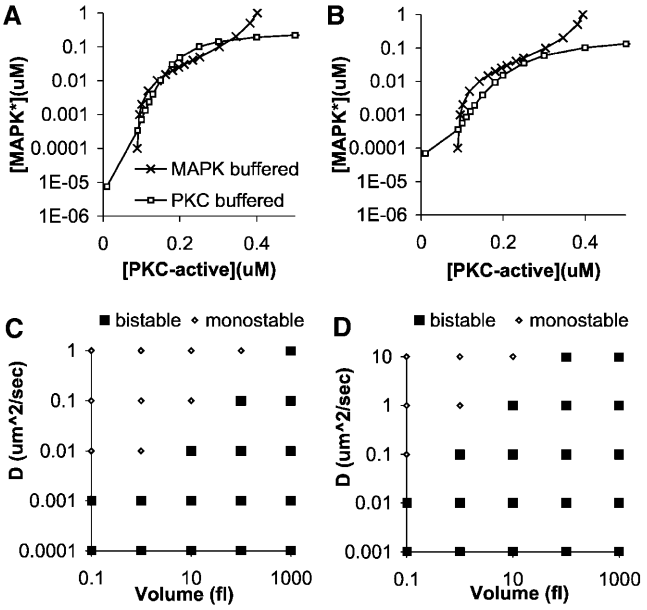

FIGURE 2 Bistability as a function of diffusion constant and volume. (*A*) Intersection curve for mutual dose-response plots for MAPK and PKC. MAPK* represents the active, doubly phosphorylated form of MAPK. The intersection points define stable points of the system. This model is at volume = 1 fl, and $D = 0.001\ \mu m^2/s$. There are three intersection points, hence this system is bistable. (*B*) Similar curve for volume = 1 fl, and $D = 0.01\ \mu m^2/s$. There is a single intersection point and the model is singly stable. (*C*) Conditions for bistability for compartment protruding directly from bulk. (*D*) Conditions for bistability for spine geometry.

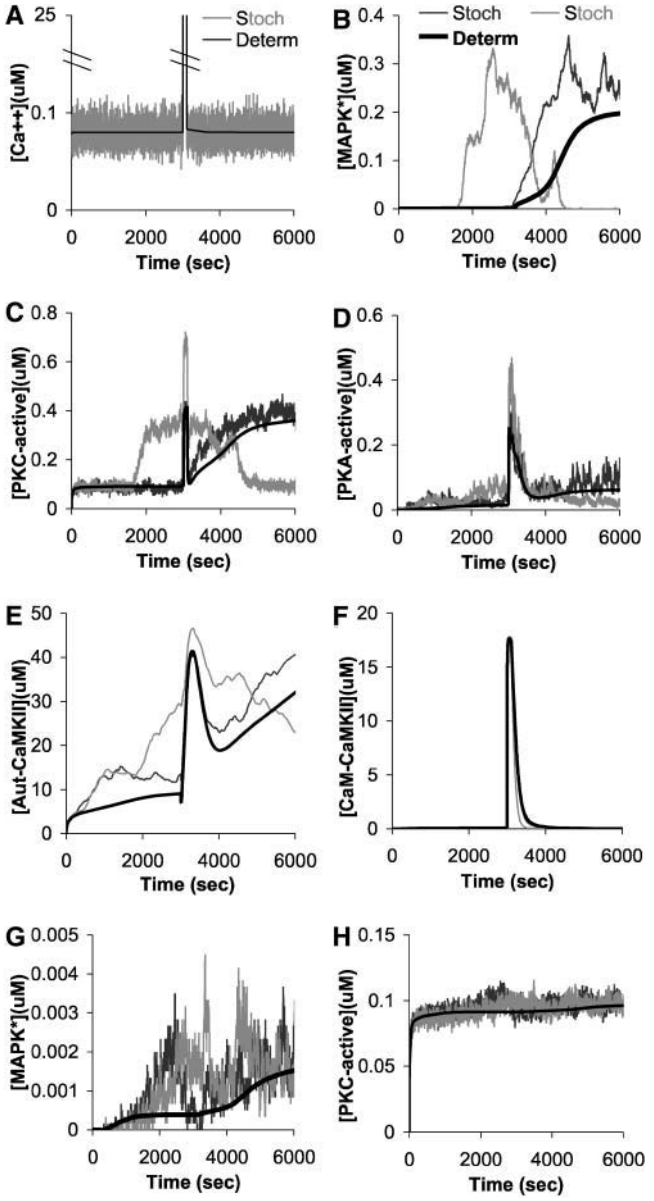

FIGURE 3 Responses of network to Ca^{2+} input of 25 μM for 100 s. Simulations used spine geometry with head volume = 1 fl, dendrite volume 10 fl, and $D = 0.1\ \mu m^2/s$. (*A*) Ca^{2+} stimulus. (*B*) Illustrative responses for MAPK*. The stimulus is suprathreshold for the deterministic model (*thick line*) but in the stochastic case there may be spontaneous turn-on with washout (*light shaded*) or stimulus-triggered turn-on. The same two simulation runs were used to illustrate responses of other pathways. (*C*) PKC response. (*D*) PKA response. (*E*) Autonomous CaMKII (phosphorylated on Thr-305). Note that the CaMKII response does not settle in the time course of the simulation for both runs where the MAPK activity remains elevated. (*F*) Ca-CaM activated response of CaMKII. (*G*) MAPK response in the dendrite. There is some propagation of activity from the spine head to the dendritic compartment. (*H*) PKC response in the dendrite. All runs nearly overlap.

The above approach for assessing bistability is not useful for stochastic calculations as the convergence to steady state, required for dose-response curves, is not applicable when the system exhibits large stochastic fluctuations. To address bistability in the synaptic geometry, a large, suprathreshold Ca^{2+} stimulus (25 μM/100 s) was applied to the model after a settling time of 3000 s, and the time-evolution of levels of signaling molecules were monitored. This Ca^{2+} stimulus itself was stochastic (Fig. 3 *A*). Not surprisingly, the outcome of each stochastic run was different. Interestingly, the synaptic system often exhibited spontaneous excursions into the upper stable state even before the stimulus was applied. Further, there were frequent collapses of activity from the high state back down to the low activity state (Fig. 3 *B*).

Different signaling pathways exhibit different levels of stochasticity. Whereas PKC and PKA have roughly comparable levels of high frequency stochastic noise, autonomous CaMKII and MAPK appear to have lower frequency noise but large percentage excursions (Fig. 3, *B–E*). In both cases there are several stages of phosphorylation between the initial Ca^{2+} stimulus and the response, which may act as a temporal filter and amplifier. CaM-bound CaMKII responses have very small stochastic variability (Fig. 3 *F*). As the ''bulk'' dendrite volume in these runs was only 1 fl, it too exhibited stochastic fluctuations (Fig. 3, *G* and *H*). The coupling between spine and bulk leads to a small but distinct increase in MAPK and PKC activity in the dendrite in the deterministic case. This increase is also present but obscured by noise in the stochastic case (Fig. 3, *G* and *H*).

As analyzed in Fig. 2, the responses to synaptic stimulation can be bistable or not, depending on the diffusion constant as well as volume. This is seen in the time course of response of MAPK to the same 25 μM/100 s Ca^{2+} stimulus in deterministic runs (Fig. 4 *A*). When the stimulus is suprathreshold, the activation may propagate into the dendritic compartment under suitable diffusion conditions (Fig. 4 *B*). This propagation crosses the turn-on threshold for the feedback loop if the dendritic compartment is small enough (e.g., 0.5 fl with $D = 0.01$ $\mu m^2/s$, data not shown). These simple effects are nearly obscured when stochasticity is considered. Spontaneous turn-on and turnoff are common, both in the spine and dendrite. In many cases it appears that the spontaneous turn-on in the spine may be followed by turn-on in the dendrite (Fig. 4 *C*, but see *D* and *G* for counterexamples). The turn-on may occur even if the system is not in the nominal bistable regime as defined by stochastic calculations in Fig. 2. In Fig. 4 *E*, the 0.01 $\mu m^2/s$ case is bistable, whereas the 0.1 $\mu m^2/s$ case is not, but both exhibit clear excursions to high activity states of ~0.4 μM of MAPK*. In such cases it appears that the stochastic diffusion of molecules to or from the spine may occasionally switch the instantaneous environment from one favoring low activity to one with high activity, thus permitting MAPK turn-on even in nonbistable conditions. The presence of high dendritic activity can also affect the noise profile of MAPK activity in the spine through diffusion (Fig. 4 *G*). Here the spine MAPK activity fluctuates but at a rather low rate as long as the dendritic activity is low. As soon as the dendrite switches ''on'', the noise in the spine MAPK becomes larger even though there is no obvious effect on average activity in the spine.

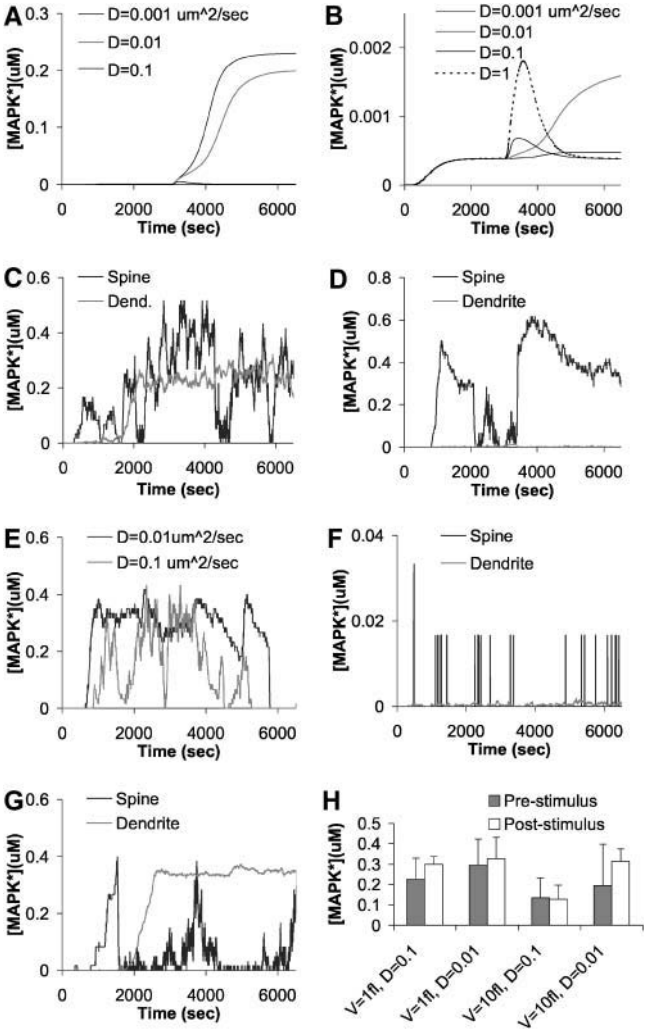

FIGURE 4 Different kinds of network responses to 25 μM Ca^{2+} stimulus delivered for 100 s. (*A*) Deterministic response in the spine with head volume $Vhead = 0.1$ fl and dendrite volume $Vdend = 1$ fl. (*B*) Deterministic responses in the dendrite of the same spine. (*C*) Stochastic run, same spine geometry, $D = 0.1$ $\mu m^2/s$. Spine activation followed by dendritic activation of MAPK activity. (*D*) Stochastic run, same spine geometry, $D = 0.01$ $\mu m^2/s$. Spine activation without propagation into dendrite. (*E*) Comparison of MAPK responses in bistable (0.01 $\mu m^2/s$) and singly stable (0.1 $\mu m^2/s$) regimes, same spine geometry except that the $Vdend = 10$ fl in the second plot. Despite the lack of bistability and larger dendrite volume in the second plot, the two curves have similar peak amplitudes. (*F*) Response at $Vhead = 0.1$ fl, $Vdend = 10$ fl, and $D = 1$ $\mu m^2/s$, where neither spine nor dendrite is stimulated into high-activity state. (*G*) Diffusive influences on chemical noise in synapse. $Vhead = 0.1$ fl, $Vdend = 0.5$ fl, and $D = 0.01$ $\mu m^2/s$. The spine response has infrequent stochastic transitions whereas the dendrite is inactive, but becomes very noisy when the dendrite turns on. (*H*) Comparison of mean responses for 1000 s before and 2800 s after stimulus. The network exhibits little long-term change after the stimulus.

How well does such a noisy bistable system ''remember'' the Ca^{2+} stimulus? Means before and after the stimulus are compared in Fig. 4 *H*, and it is clear that the standard deviation of the responses is much larger than any difference between the prestimulus and poststimulus averages. Under the assumptions of this model, an individual synapse has very little ''memory'' of the Ca^{2+} transient when stochasticity is considered, even when deterministic calculations suggest it should be bistable.

Thresholding

An important computational function of bistable systems is thresholding with hysteresis (Bhalla and Iyengar, 2001; Bhalla et al., 2002). We investigated thresholding using the model geometry where a compartment of defined volume is adjacent to a bulk compartment of 1000 fl. This configuration was chosen to explore a wide range of compartment volumes. As discussed in the methods section, in the small-volume low diffusion limit, effects with this geometry are equivalent to those in the synaptic spine. The thresholding function is complicated by diffusion, where the washout of active molecules introduces a time-dependence on threshold and activity levels. Here the threshold appears to be between 0.12 and 0.15 μM Ca^{2+}. Introduction of stochasticity considerably blurs the concept of thresholding as the system fluctuates between the low and high activity states (Fig. 5 *A*). At higher diffusion rates the threshold for bistability is

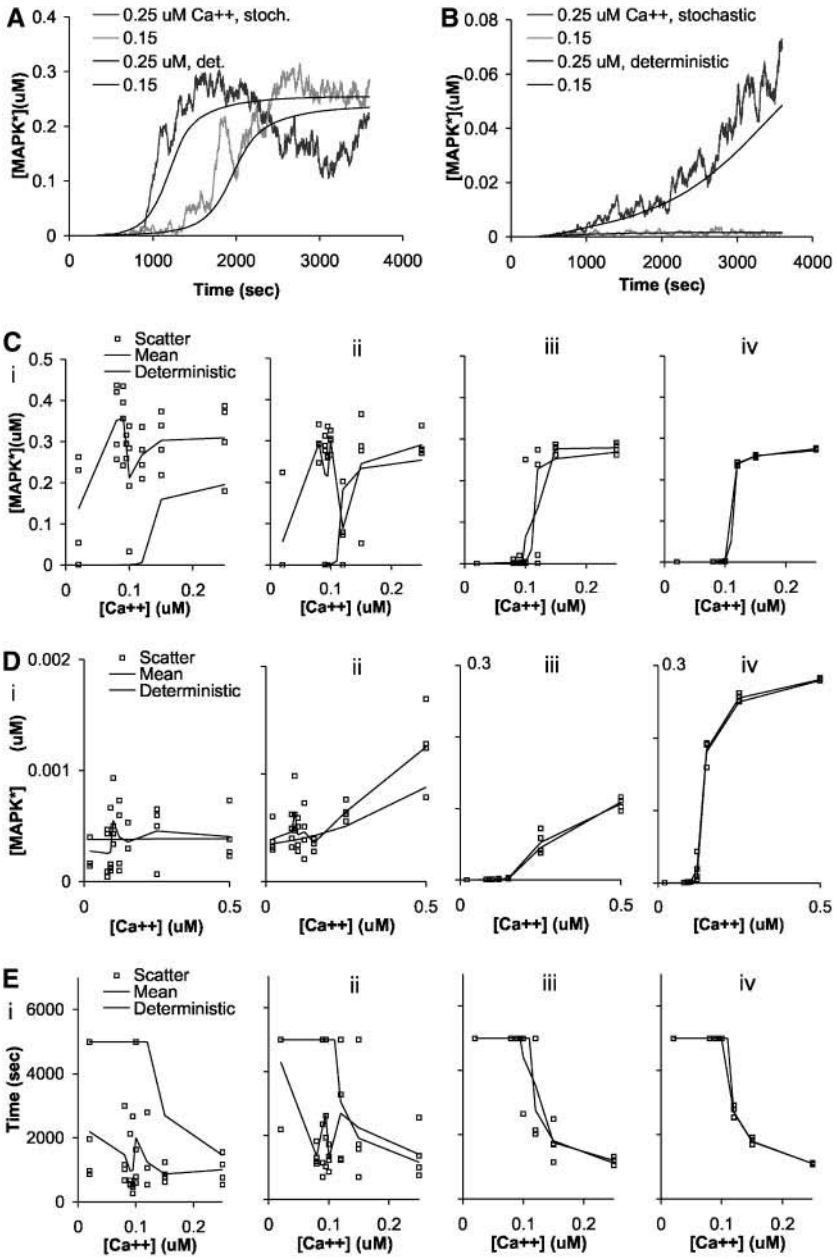

FIGURE 5 Responses to steady Ca^{2+} inputs of different amplitudes, using small compartment attached to bulk volume of 1000 fl. (*A*) Illustrative runs for volume = 1 fl and $D = 0.001\ \mu m^2/s$, at different Ca levels. The smooth curves are deterministic simulations. Note the large difference between simulated and deterministic runs under the same conditions. (*B*) Similar runs for volume = 100 fl and $D = 0.1\ \mu m^2/s$. The stochastic curves follow the deterministic ones much more closely. (*C*) Averaged peak responses as a function of Ca^{2+} for $D = 0.001\ \mu m^2/s$ and a range of compartment volumes: *i*, 01 fl; *ii*, 1 fl; *iii*, 10 fl; and *iv*, 100 fl. (*D*) Similar responses but for $D = 0.1\ \mu m^2/s$. (*E*) Time until turn-on of MAPK response, as determined by its first crossing of 0.1 μM. Failure to turn on is represented as a value of 5000 s. The thin line is the mean of the individual stochastic runs and the thick line the deterministic outcome. Simulations at same range of compartment volumes, $D = 0.001\ \mu m^2/s$.

higher, and the same Ca^{2+} levels may cause only a small elevation in activity (Fig. 5 *B*). Interestingly the stochastic curves track the deterministic ones more closely under high-diffusion conditions, because the positive feedback loop is no longer able to amplify fluctuations to the same extent.

The effect of volume on stochasticity and thresholding was examined by taking a series of compartment volumes and measuring simulated peak responses. The peak was computed by numerically finding the largest response and then averaging the samples for ± 250 s around this peak. The peak measurement rather than long-term settled level of MAPK was chosen for this measurement since the responses are transient in many cases (e.g., Fig. 5 *A*). The 500-s average was taken as a representation of the chemical averaging expected from the kinetics of a downstream target of MAPK*. Using this approach, MAPK* responses were assessed for diffusion constants of $0.001\ \mu m^2/s$, (Fig. 5 *C*) and $0.1\ \mu m^2/s$ (Fig. 5 *D*). The former is bistable under deterministic conditions and the latter is singly stable except for the case with the largest volume of 100 fl (Figs. 2 and 5 *D iv*). Three effects stand out in the thresholding calculations. First, as expected, the stochastic runs converge to the deterministic case at large volumes (Fig. 5 *C iv*). Second, the Ca^{2+} dependent thresholding process is converted into a Ca^{2+} dependent probability of MAPK* activation. At low Ca^{2+} levels there is a low probability of MAPK* turning on.

Near the threshold the probability rises and there is a scatter of points both with high and low activities. At high Ca^{2+} levels most runs are in the high MAPK* state. Third, at small volumes, the spontaneous ''on'' transitions become so frequent as to obscure the Ca^{2+} dependence.

When the system is no longer bistable, the thresholding effect is lost (Fig. 5 *D*). As before, the stochastic responses cluster more closely around the deterministic case at increasing volumes. The previously observed elevation of response baseline due to spontaneous ''on'' responses is much smaller here (Fig. 5 *D*, *i* and *ii*) than when bistability is present (Fig. 5 *C*, *i* and *ii*).

A further measure of stochastic effects on thresholding is to consider the time it takes for the system to make the transition to the active state. The time of first ''on'' transition was measured as the time taken for the MAPK* activity to cross 0.1 μM (Fig. 5 *E*). Depending on stimulus levels, the MAPK* level may never reach 0.1 μM, and this situation was scored as a maximal time of 5000 s. At small volumes there is a sharp distinction between deterministic and stochastic runs (Fig. 5 *E*, *i*). The deterministic model may never turn on, or only turn on at a very late time point if Ca^{2+} levels are high. In contrast, almost all the stochastic runs do turn on at some point during the simulation, regardless of Ca^{2+} input levels. At larger volumes the chance of spontaneous turn-on is lower at low Ca^{2+}. As expected, higher Ca^{2+} levels lead to a more rapid turn-on in cases where bistability is present. This effect is evident for all the deterministic runs and the large-volume stochastic runs. At very large volumes the two cases converge.

Inspection of the scatter of MAPK* levels in Fig. 5 suggested that the presence of stochasticity introduced a distribution of responses which was bimodal in the presence of bistability. This was analyzed by constructing frequency histograms of MAPK* levels sampled at 1 s from 3000 to 3600 s after the start of each stochastic run. This time-interval was chosen as the deterministic curves had mostly settled to near their peak values at these times (Fig. 5 *A*). Histograms were constructed for volumes of 0.1 to 100 fl, using a diffusion constant of 0.001 $\mu m^2/s$, for three Ca stimulus values selected to be below, near, and above the threshold (Fig. 6, *A–D*). At 0.1 fl the responses to the three stimuli are indistinguishable and there is a very long tail of MAPK activity (Fig. 6 *A*). At increasing volumes the distribution of MAPK activities into high and low states becomes sharper. By 10 fl the low (0.08 μM Ca^{2+}) and high (0.25 μM Ca^{2+}) stimuli each elicit unimodal responses, and the near-threshold stimulus of 0.12 μM Ca^{2+} is distinctly bimodal (Fig. 6 *C*). As considered in the discussion, this partitioning of MAPK* levels into the upper and lower activity states is analogous to a thermodynamic distribution of a system into a state with two energy minima separated by a barrier. At the high diffusion rate of 0.1 $\mu m^2/s$, the distributions are much narrower and simply reflect whether the system is singly stable or bistable (supplementary material).

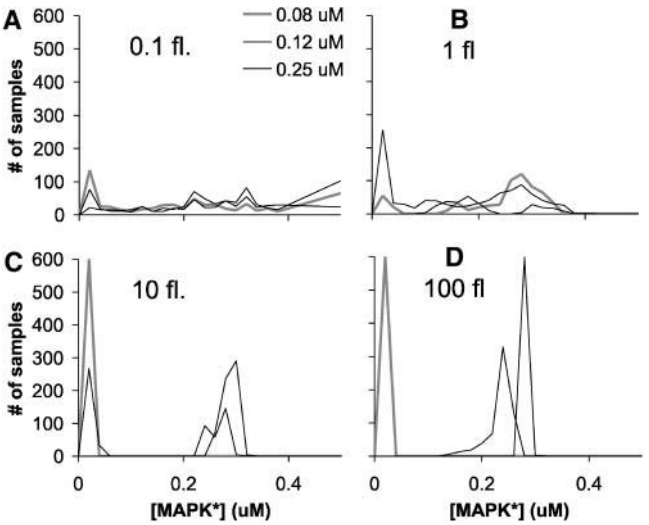

FIGURE 6 Histograms of distribution of MAPK activities for different volumes and Ca^{2+} levels. Diffusion constant = 0.001 $\mu m^2/s$. Volumes are indicated in the figure. In *A* and *B* the histograms are averages of eight independent runs, taking 600 samples from each, sampling at 1 point per second starting 3000 s after the stimulus input. In *C* and *D*, four runs are averaged, again with 600 sample points from each. The nearly uniform distribution at low volumes gives way to a strongly biphasic distribution at large volumes, reflecting the reduced likelihood of stochastic transitions between states.

Temporal tuning

Nondiffusive deterministic analyses of this signaling network have previously shown that it is capable of a range of temporal tuning properties (Bhalla, 2002a,b). To analyze tuning we used a similar stimulus to that adopted in the previous studies. The stimulus consisted of a 1-s Ca^{2+} pulse of 25 μM, separated by different interpulse intervals from 10 to 1800 s (Fig. 7 *A*). The pulses were applied after an initial settling period of 3000 s. As a measure of integrated response for selected pathways, the activity was averaged for 3000 s from the start of the first pulse. Simulations were performed both with the synaptic spine geometry and also using a small compartment attached to the bulk cytosolic volume of 1000 fl. Typical response time courses for PKC and MAPK are illustrated in Fig. 7, *B* and *C,* for compartment volumes of 10 and 0.1 fl, respectively, and a diffusion constant of 0.001 $\mu m^2/s$. The stochastic tuning curves for MAPK* show a striking departure from the deterministic ones (Fig. 7). At 10 fl compartment size (Fig. 7 *D*) the stochastic responses are bimodal as seen in Fig. 6, and the high activity of the activated MAPK* state raises the average stochastic response nearly two orders of magnitude above the deterministic response. Temporal tuning is not evident here.

An interesting effect analogous to stochastic resonance is observed at 100 fl compartment size. In this case there are a small number of transitions to the active state, and their probability is greater around 600 s interpulse interval. The high activity of the ''on'' state amplifies the tuning nearly 10-fold compared to the deterministic case. In the spine

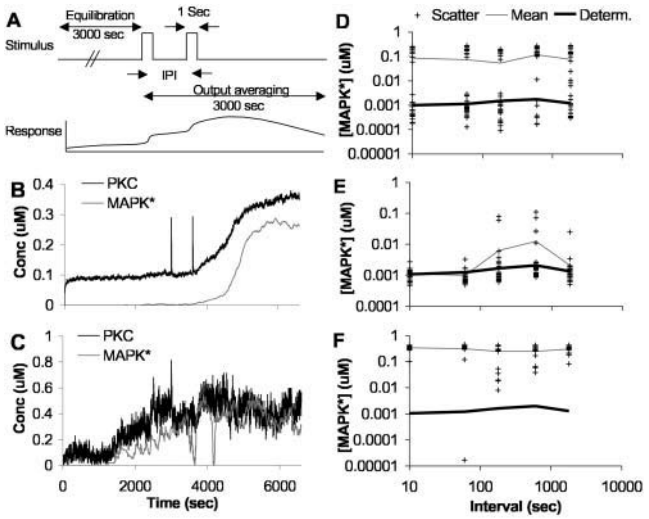

FIGURE 7 Interpulse interval tuning. (*A*) Stimulus protocol. Two 1-s pulses of 25 μM Ca^{2+} were separated by IPIs from 10 to 1800 s. The response was averaged for 3000 s after the start of the stimulus. (*B*) Responses of MAPK and PKC for $IPI = 600$ s, volume = 10 fl, and $D = 0.001$ $\mu m^2/s$. (*C*) Responses of MAPK and PKC for $IPI = 600$ s, volume = 0.1 fl, and $D = 0.001$ $\mu m^2/s$. (*D–F*) Deterministic and stochastic temporal tuning responses. $D = 0.001$ $\mu m^2/s$ in each case. (*D*) Compartment geometry, volume = 10 fl. Stochastic response is bimodal, and mean is above deterministic mean. (*E*) Compartment geometry, volume = 100 fl. Stochastic-resonance like amplification of response for selected IPIs. (*F*) Synapse geometry, head volume $Vhead = 0.1$ fl, and dendrite volume $Vdend = 1$ fl. Most stochastic responses are elevated with respect to baseline.

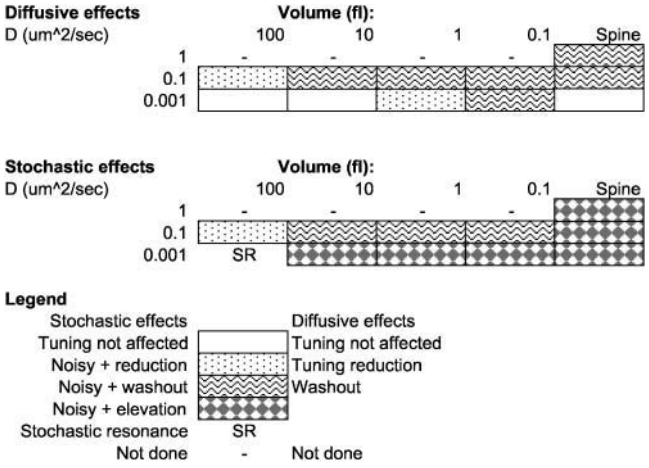

FIGURE 8 Summary of stochastic and diffusive effects on interpulse-interval tuning. Four volumes are considered for the case of a subcellular compartment coupled to a 1000 fl cell, and in the case of the synaptic spine a volume of 0.1 fl is coupled to a 1 fl dendritic compartment. Diffusive effects, as expected, lead to washout of the tuning response especially at high diffusion rates and small volumes. Stochasticity introduces spontaneous elevation of MAPK activity due to molecular noise and positive feedback, when diffusion rates are small. In a subset of conditions of moderate stochastic noise and low diffusion, stochastic amplification is observed.

geometry (0.1 fl spine head and 1 fl dendrite, Fig. 7 *F*) the spontaneous turn-ons again raise the average activity well above the deterministic value, and tuning is lost.

How robust is temporal tuning when diffusive contexts and stochasticity are considered? Tuning curves were computed for MAPK* in a range of diffusive contexts and compared with and without stochasticity. The results are summarized in Fig. 8 and presented in detail in the supplementary material. Diffusion and stochasticity both diminish the fidelity of tuning, sometimes with opposing effects on the baseline response. Diffusion tends to give rise to washout of the response, and stochasticity may elevate the baseline activity when feedback effects are large (e.g., Fig. 7 *F*). In a limited range of conditions, stochastic resonance leads to a large enhancement of tuning (e.g., Fig. 7 *E*). Temporal tuning profiles of other pathways undergo similar degradation due to diffusive washout and stochasticity (supplementary material). Under the assumptions of this study, only CaM-activated CaMKII tuning was still evident in the synaptic spine.

DISCUSSION

This article has analyzed three computational functions that are emergent properties of the synaptic signaling network: bistability, thresholding, and pattern selectivity. The effects of diffusion and stochasticity have been considered for several pathways, with special attention to the dendritic spine geometry and a feedback loop involving the MAPK pathway. Both diffusion and stochasticity set strong limits to the kinds of computation possible using conventional reaction-diffusion assumptions about signaling. In particular, diffusion leads to washout of many signaling responses at interesting timescales, and stochastic chemical noise obscures most responses on synaptic volume scales. The simulations also uncover an interesting potential stochastic resonance-like effect that may actually enhance temporal tuning.

Diffusive washout

The dendritic spine is believed to be a subcellular compartment which is relatively diffusively isolated from the dendrite (Svoboda et al., 1996). On short timescales this is clearly the case, but many of the key functions of synapses occur in the range of tens of minutes. These include pattern selectivity, the transition between different phases of synaptic potentiation, and synaptic remodeling (Soderling and Derkach, 2000; Wu et al., 2001). Many other signaling networks are also localized in small compartments or microdomains (Rich et al., 2000; Hur and Kim, 2002) and are also likely to be subject to diffusive turnover according to our calculations. An obvious mechanism to prevent diffusive washout is to anchor molecules to the cytoskeleton or membrane. The calculations in the current study took many such known anchoring situations into account by defining appropriate molecules as

nondiffusing. I suggest two additional mechanisms that may preserve signaling networks despite diffusive interchange. The first is simply the presence of unidentified diffusive barriers and cytoskeletal anchoring molecules that reduce diffusion rates by 10- to 100-fold in specific microdomains. Such barriers and anchors could involve relatively weak, nonspecific interactions and thus may be hard to identify. Much tighter diffusive barriers have in fact already been proposed based on direct experimental observations (Rich et al., 2000). Such diffusively restricted domains might not show up when conventional measurements of diffusion are done using particle tracking. Fluorescence correlation spectroscopy may be able to identify such diffusive constraints in microdomains, but only if the diffusive barriers are within the volume range ($\sim$1 fl) of the fluorescence correlation spectroscopy spot (Haustein and Schwille, 2003). The second proposed mechanism is the presence of active transport and recruitment processes. The timescale of many neuronal transport processes is of the order of minutes (Horton and Ehlers, 2003), and this is similar to the time range that these simulations suggest would be susceptible to washout. It will be necessary to obtain a considerably more detailed knowledge of cell biological events in cellular subdomains to assess the role of such mechanisms.

Stochastic noise

As expected from the results in the accompanying article, stochastic noise obscures signal in small signaling volumes. This result is particularly stark for the simulations of the dendritic spine, where most signaling outputs are obscured. Only one highly abundant signaling molecule (CaMKII), activated in turn by another abundant protein (CaM) appears to provide reasonably reliable signal output at the spine. This is clearly a biologically unreasonable conclusion. Given this rather fundamental departure from observed biological behavior, and the use of relatively constrained signaling parameters, it appears that basic model assumptions rather than individual parameters are to blame. In this context, the results of this study can be interpreted as a reductio ad absurdum exercise in ruling out certain assumptions about synaptic signaling and possibly microdomain signaling in general. I propose that two key model assumptions are questionable. Both relate to scaling of test-tube chemistry to cellular microdomains and in particular to signaling complexes.

The first assumption is that one can scale molecular concentrations smoothly down to femtoliter volumes. Instead it is likely that many key molecules exist in complexes, where the local concentrations of interacting molecules may be orders of magnitude larger than their bulk concentrations. For example, members of the MAPK cascade are known to be bound to a scaffold protein that brings together proteins involved in successive stages of the cascade (Morrison and Davis, 2003). This situation is likely to be common to many of the signaling molecules of the network. There is also evidence that many kinase substrates and certain states of CaMKII may be bound to the PSD complex (Yamauchi, 2002). In all these cases, the formation of complexes may raise effective protein concentrations by orders of magnitude. By increasing the number of interacting molecules in a microdomain, this correction would substantially improve signaling fidelity.

The second assumption is that reaction mechanisms themselves are equivalent to those observed in the test tube. Here direct examples of different mechanisms at the synapse are rare. However, emerging data from other molecular complexes, such as the ribosome (Moore and Steitz, 2003) and electron-transport complexes (Paddock et al., 2003), suggests that special, nonreaction-diffusion mechanisms are biologically plausible. The cell may have evolved specific signaling mechanisms that act to reduce molecular noise. For example, DNA looping has been recently identified as a mechanism for noise reduction by providing synergistically acting sites for gene regulation (Vilar and Leibler, 2003). Another noise-reducing effect may be the proposed phenomenon of molecular brachiation in receptor arrays (Levin et al., 2002). Such properties appear to be consistent with physiological readouts of the reliability of synaptic and small-volume signaling processes, and further support the idea that synaptic signaling may involve chemical mechanisms distinct from simple reaction-diffusion chemistry.

It is intriguing that mass-action signaling models, involving some of these same pathways, can be relatively successful in replicating and predicting many properties of bulk cellular signaling (Bhalla et al., 2002). Further, the in vivo properties of synaptic pathways appear to be reasonably consistent with their bulk properties as determined by knockout and pharmacological experiments (Blitzer et al., 1998; Zeng et al., 2001). These observations may provide some useful constraints for future experimental and simulation work to identify small-volume signaling mechanisms.

Stochastic resonance and tuning amplification

Although the primary results of these simulations has been to highlight the constraints on signaling imposed by small volumes, the results also point to a situation where stochasticity can actually enhance a signaling computation (Figs. 7 and 8). In this case, a small underlying tuning effect is enhanced by the presence of stochasticity to give a much sharper (high Q) tuning. It is interesting that this effect arises from all three of the computational properties examined in this study: bistability, thresholding, and temporal tuning. The mechanism is similar to that of stochastic resonance (Collins et al., 1995) in that the underlying system response is subthreshold, and the chemical noise raises a fraction of the runs above threshold. However, the amplification effect in this context is provided not only because the active state is

considerably higher than baseline, but also because the system is bistable and hence the elevated activity persists for a prolonged period. The amplification depends strongly on the volume. In a thermodynamic sense, a larger volume is analogous to a reduction in temperature, because the ''noise'' is reduced. The partitioning of the system into upper and lower states depending on volume is illustrated in Fig. 6. Although these simulations predict a rather large volume ($\geqslant$10 fl) for the effect of stochastic amplification of tuning, it seems plausible that correction of the model assumptions for local concentrations may bring such stochastic resonance effects into play in physiological settings.

SUPPLEMENTARY MATERIAL

An online supplement to this article can be found by visiting BJ Online at http://www.biophysj.org.

The author acknowledges the programming work by Karan Vasudeva in implementing numerical methods used in this project, and useful comments by J. Mishra and S.M. Ajay.

This work was supported by funds from National Centre for Biological Sciences, Tata Institute of Fundamental Research, and an International Senior Research Fellowship from the Wellcome Trust to U.S.B.

REFERENCES

Abeliovich, A., C. Chen, Y. Goda, A. Silva, C. F. Stevens, and S. Tonegawa. 1993. Modified hippocampal long-term potentiation in PKC gamma-mutant mice. *Cell*. 75:1253–1262.

Bhalla, U. S. 1998. The Network Within: Signaling Pathways. *In* The Book of GENESIS: Exploring Realistic Neural Models with the GEneral NEural SImulation System. J. M. Bower and D. Beeman, editors. Springer-Verlag, New York. 169–190.

Bhalla, U. S. 2002a. Mechanisms for temporal tuning and filtering by postsynaptic signaling pathways. *Biophys. J.* 83:740–752.

Bhalla, U. S. 2002b. Temporal pattern decoding by synaptic signaling pathways. *J. Comput. Neurosci.* 13:49–62.

Bhalla, U. S. 2002c. Use of Kinetikit and GENESIS for modeling signaling pathways. *In* Methods in Enzymology. J. D. Hildebrandt and R. Iyengar, editors. Academic Press. 3–23.

Bhalla, U. S., and R. Iyengar. 1999. Emergent properties of networks of biological signaling pathways. *Science*. 283:381–387.

Bhalla, U. S., and R. Iyengar. 2001. Robustness of the bistable behavior of a biological signaling feedback loop. *Chaos*. 11:221–226.

Bhalla, U. S., P. T. Ram, and R. Iyengar. 2002. MAP Kinase phosphatase as a locus of flexibility in a mitogen-activated protein kinase signaling network. *Science*. 297:1018–1023.

Bialek, W. 2001. Stability and noise in biochemical switches. *NIPS*. 13: 103–109.

Blitzer, R. D., J. H. Connor, G. P. Brown, T. Wong, S. Shenolikar, R. Iyengar, and E. M. Landau. 1998. Gating of CaMKII by cAMP-regulated protein phosphatase activity during LTP. *Science*. 280:1940–1942.

Bolshakov, V. Y., L. Carboni, M. H. Cobb, S. A. Siegelbaum, and F. Belardetti. 2000. Dual MAP kinase pathways mediate opposing forms of long-term plasticity at CA3–CA1 synapses. *Nat. Neurosci.* 3:1107–1112.

Bray, D. 2001. Cell Movements: from Molecules to Motility. Garland Publishing, New York.

Collins, J. J., C. C. Chow, and T. T. Imhoff. 1995. Stochastic resonance without tuning. *Nature*. 376:236–238.

Haustein, E., and P. Schwille. 2003. Ultrasensitive investigations of biological systems by fluorescence correlation spectroscopy. *Methods*. 29:153–166.

Horton, A. C., and M. D. Ehlers. 2003. Neuronal polarity and trafficking. *Neuron*. 40:277–295.

Hur, E. M., and K. T. Kim. 2002. G protein-coupled receptor signalling and cross-talk: achieving rapidity and specificity. *Cell. Signal.* 14:397–405.

Levin, M. D., T. S. Shimizu, and D. Bray. 2002. Binding and diffusion of CheR molecules within a cluster of membrane receptors. *Biophys. J.* 82:1809–1817.

Lisman, J. E., and M. A. Goldring. 1988. Feasibility of long-term storage of graded information by the Ca2+/calmodulin-dependent protein kinase molecules of the postsynaptic density. *Proc. Natl. Acad. Sci. USA*. 85: 5320–5324.

Lisman, J. E., and C. C. McIntyre. 2001. Synaptic plasticity: a molecular memory switch. *Curr. Biol.* 11:R788–R791.

Moore, P. B., and T. A. Steitz. 2003. The structural basis of large ribosomal subunit function. *Annu. Rev. Biochem.* 72:813–850.

Morrison, D. K., and R. J. Davis. 2003. Regulation of MAP kinase signaling modules by scaffold proteins in mammals. *Annu. Rev. Cell Dev. Biol.* 19:91–118.

Paddock, M. L., G. Feher, and M. Y. Okamura. 2003. Proton transfer pathways and mechanism in bacterial reaction centers. *FEBS Lett.* 555:45–50.

Rich, T. C., K. A. Fagan, H. Nakata, J. Schaack, D. M. Cooper, and J. W. Karpen. 2000. Cyclic nucleotide-gated channels colocalize with adenylyl cyclase in regions of restricted cAMP diffusion. *J. Gen. Physiol.* 116:147–161.

Selcher, J. C., E. J. Weeber, J. Christian, T. Nekrasova, G. E. Landreth, and J. D. Sweatt. 2003. A role for ERK MAP Kinase in physiologic temporal integration in hippocampal area CA1. *Learn. Mem.* 10:26–39.

Sheng, M., and M. J. Kim. 2002. Postsynaptic signaling and plasticity mechanisms. *Science*. 298:776–780.

Sivakumaran, S., S. Hariharaputran, J. Mishra, and U. S. Bhalla. 2003. The database of quantitative cellular signaling: repository and analysis tools for chemical kinetic models of signaling networks. *Bioinformatics*. 19:408–415.

Soderling, T. R., and V. A. Derkach. 2000. Postsynaptic protein phosphorylation and LTP. *Trends Neurosci.* 23:75–80.

Svoboda, K., D. W. Tank, and W. Denk. 1996. Direct measurement of coupling between dendritic spines and shafts. *Science*. 272:716–719.

Tsodyks, M. 2002. Spike-timing-dependent synaptic plasticity—the long road towards understanding neuronal mechanisms of learning and memory. *Trends Neurosci.* 25:599–600.

Vasudeva, K., and U. S. Bhalla. 2004. Adaptive stochastic-deterministic chemical kinetic simulations. *Bioinformatics*. 20:78–84.

Vilar, J. M. G., and S. Leibler. 2003. DNA looping and physical constraints on transcription regulation. *J. Mol. Biol.* 331:981–989.

Weiss, M., H. Hashimoto, and T. Nilsson. 2003. Anomalous protein diffusion in living cells as seen by fluorescence correlation spectroscopy. *Biophys. J.* 84:4043–4052.

Wu, G.-Y., K. Deisseroth, and R. W. Tsien. 2001. Spaced stimuli stabilize MAPK pathway activation and its effects on dendritic morphology. *Nat. Neurosci.* 4:151–158.

Yamauchi, T. 2002. Molecular constituents and phosphorylation-dependent regulation of the post-synaptic density. *Mass Spectrom. Rev.* 21: 266–286.

Zeng, H., S. Chattarji, M. Barbarosie, L. Rondi-Reig, B. D. Philpot, T. Miyakawa, M. F. Bear, and S. Tonegawa. 2001. Forebrain-specific calcineurin knockout selectively impairs bidirectional synaptic plasticity and working/episodic-like memory. *Cell*. 107:617–629.